

Vibrations of Circular Orthotropic Plates in Affine Space

Gabriel A. Oyibo*

Fairchild Republic Company, Farmingdale, New York

and

Eugene J. Brunelle†

Air Force Institute of Technology, Wright-Patterson Air Force Base, Ohio

The vibration of an initially compressed plate having a circular geometry and orthotropy is examined in an affine space. Classical linear plate theory and the Hamilton's principle are employed. The plate's equations of motion are particularly simple in the chosen affine space, permitting a free vibration study of the entire composite materials having polar orthotropy. Approximate, but very accurate, standing-wave-type mode shapes are utilized in solving the essentially double eigenvalue problem to determine the effects of midplane forces on the vibration frequencies of the plate. The results indicate that the affine space frequency increases with increasing stiffness ratio $D_{\theta r}^*$ but decreases with increasing midplane compression. It is also discovered that, contrary to the trends observed by the authors in previous investigations for rectangular geometry and orthotropy, the affine space frequency increases with increasing generalized Poisson's ratio ϵ_r .

Nomenclature

\bar{a}_n	= coefficients of r_0^n
h, a	= plate thickness and radius, respectively
$k_{\theta r}$	= stability (buckling) coefficients in polar affine space
r, θ	= polar orthotropic coordinates
r_0, θ	= polar affine space
t_n	= quantities defined for computational purposes
$D_{\theta r}^*$	= generalized rigidity ratio in polar affine space
D_{ij}	= elastic constants
N_{ij}	= initial stress in polar orthotropic coordinates
U_r	= virtual work in polar orthotropic coordinates
U_{r_0}	= virtual work in polar affine space
w, W	= mode shapes
ϵ_r	= generalized Poisson's ratio in polar affine coordinates
ω	= angular frequency of vibration
ω_0	= vibration frequency parameter in polar affine space
$\rho_{\theta r}$	= density of plate in polar affine coordinates

Introduction

THE problems of determining the natural vibration frequencies and the buckling forces for circular anisotropic plates having polar orthotropy have received a great deal of attention from numerous investigators, e.g., Refs. 1-8. While the polar orthotropy reduces the number of elastic constants (which should result in a simplification of the problem) the circular geometry makes it necessary to expect the exact solutions (mode shapes) in terms of hypergeometric functions of which Bessel functions are a subset. Therefore, it did not come as a total surprise when von Woinowsky-Krieger,⁴ in his analysis, found the exact closed-form solution to the buckling problem in terms of Bessel functions. However, the vibration problem seems to lack known exact closed-form solutions except for an isotropic case. Hence, approximate methods of solution are resorted to.

It must be pointed out that a number of investigators tried to minimize the number of elastic constants in the problems by dividing both sides of the equations of motion by one of the elastic constants. In the process, parameters wholly or partially equivalent to those of the present analysis are defined. Interestingly enough, no one seemed to realize that these parameters are the key to presenting the trends for all composite materials having a circular geometry and orthotropy, thereby permitting a convenient comparison of candidate material for a particular application.

The present investigation stems from the previous efforts by the authors¹⁰⁻¹³ in which problems of plates having a rectangular geometry and orthotropy were successfully studied in affine space. The present analysis, therefore, attempts to employ a similar approach to study the vibration problem of initially compressed plates having a circular geometry and orthotropy to determine the trends for all materials and, as a byproduct, establish any differences between polar and rectangular orthotropies and geometries. Hence, by affinely stretching the radial coordinate, the equations of motion are simplified, resulting in the definition of two bounded generic variables, $D_{\theta r}^*$ and ϵ_r , called the generalized rigidity ratio and generalized Poisson's ratio, respectively. Consequently, the essentially double eigenvalue problem is solved using approximate energy methods together with rather accurate polynomial mode shapes. A variation of $D_{\theta r}^*$ between zero and one makes it possible to present the results for all materials ($D_{\theta r}^* = 1$, corresponding to the isotropic case). The generated data expose certain unknown trends and confirm expected ones. For example, the lowest symmetric natural frequency is seen to decrease with increasing compression at the edge, and, where applicable, increases with increasing generalized Poisson's ratio (a reverse of the trend observed for a rectangular geometry and orthotropy¹¹⁻¹³).

Problem Statement

Consider an initially compressed plate having a circular geometry and orthotropy, whose elemental idealization is shown in Fig. 1. The plate has a thickness of h and radius of a .

Physical Space Equations of Motion

By prescribing small displacements and using variational principles or a Newtonian approach the familiar plate equation of motion and the corresponding virtual work ex-

Received Nov. 23, 1983; revision received March 2, 1984. Copyright © by G. A. Oyibo and E. J. Brunelle. Published by the American Institute of Aeronautics and Astronautics with permission.

*Senior Research and Development Engineer, Flutter and Vibrations.

†Professor, Aeronautical Engineering Department. Member AIAA.

pression in physical space are given by

$$D_r \left(r \frac{\partial^4 w}{\partial r^4} + 2 \frac{\partial^3 w}{\partial r^3} \right) - D_\theta \left(\frac{1}{r} \frac{\partial^2 w}{\partial r^2} - \frac{1}{r^2} \frac{\partial w}{\partial r} \right) - N_r \left(r \frac{\partial^2 w}{\partial r^2} + \frac{\partial w}{\partial r} \right) + \rho h \ddot{w} r = 0 \quad (1)$$

$$\delta U_r = \pi \int_0^a \delta \left\{ \left[D_r \left(\frac{\partial^2 w}{\partial r^2} \right)^2 + 2 D_{r\theta} \frac{1}{r} \frac{\partial w}{\partial r} \frac{\partial^2 w}{\partial r^2} + D_\theta \left(\frac{1}{r} \frac{\partial w}{\partial r} \right)^2 + N_r \left(\frac{\partial w}{\partial r} \right)^2 + \rho h \ddot{w} w \right] r \right\} dr \quad (2)$$

Affine Space Equations of Motion

Consider the affine transformation

$$r = r_l (D_r)^{1/2} \quad (3)$$

and the nondimensionalization scheme given by

$$r_l = r_0 a_l \quad (4)$$

where a_l is the affine space radius of the plate. When Eqs. (3) and (4) are substituted into Eqs. (1) and (2), the nondimensionalized affine space equation of motion and its virtual work counterpart are given by

$$\frac{\partial^4 w}{\partial r_0^4} + \frac{2}{r_0} \frac{\partial^3 w}{\partial r_0^3} - D_{0r}^* \left(\frac{1}{r_0^2} \frac{\partial^2 w}{\partial r_0^2} - \frac{1}{r_0^3} \frac{\partial w}{\partial r_0} \right) + k_{0r} \left(\frac{\partial^2 w}{\partial r_0^2} + \frac{1}{r_0} \frac{\partial w}{\partial r_0} \right) + \rho_{0r} h \ddot{w} = 0 \quad (5)$$

$$\delta U_{r_0} = \int_0^1 \delta \left\{ \left[\left(\frac{\partial^2 w}{\partial r_0^2} \right)^2 + 2 D_{0r}^* \epsilon_r \frac{1}{r_0} \frac{\partial w}{\partial r_0} \frac{\partial^2 w}{\partial r_0^2} + D_{0r}^* \left(\frac{1}{r_0} \frac{\partial w}{\partial r_0} \right)^2 + k_{0r} \left(\frac{\partial w}{\partial r_0} \right)^2 + \rho_{0r} h \ddot{w} w \right] r_0 \right\} dr_0 \quad (6)$$

where

$$k_{0r} \triangleq \frac{-P_{r_0}}{D_{r_0}}, \quad D_{0r}^* \triangleq \frac{D_{\theta_0}}{D_{r_0}}, \quad \epsilon_r \triangleq \frac{D_{r\theta_0}}{D_{0r}^* D_{r_0}} = \frac{N_r a^2}{D_r}, \quad = \frac{D_\theta}{D_r}, \quad = \frac{D_{r\theta}}{D_{0r}^* D_r} \quad (7)$$

The virtual work expression in Eq. (6) assumes that $w(r_0, t)$ is a product of two separate functions of r_0 and t . In the absence of such an assumption, the regular Hamilton's approach would have to be used. The generic variable D_{0r}^* has a range $0 < D_{0r}^* \leq 1$ for hypostiffened materials, and $D_{0r}^* > 1$ for hyperstiffened materials, ϵ_r varies like the Poisson's ratio, and, hence, is called the generalized Poisson's ratio by the present authors. By assuming $w(r_0, t)$ to be a harmonic function of time and an arbitrary function of space and defining the following differential operators

$$\mathcal{L} \triangleq \frac{1}{r_0} \frac{d}{dr_0}, \quad \mathcal{L}_0 \triangleq \mathcal{L} r_0^2 \mathcal{L} \quad (8)$$

Eq. (5) can be written in a form that can be conveniently examined to understand its nature. Thus,

$$[\mathcal{L}_0^2 + k_{0r} \mathcal{L}_0 + (1 - D_{0r}^*) \mathcal{L}^2 - \omega_0^2] W = 0 \quad (9)$$

where

$$w(r_0, t) = W(r_0) e^{i\omega t} \quad (10)$$

ω is the natural frequency, and

$$\omega_0^2 \triangleq \rho_{0r} h \omega^2, \quad \rho_{0r} = \rho_{\alpha} / D_r \quad (11)$$

From Eqs. (8) and (9) it can be seen that, if $D_{0r}^* = 1$ (isotropic case), \mathcal{L}_0 is clearly a Bessel operator, suggesting that the exact solution of Eq. (9) should be in terms of Bessel functions.^{7,14} It also means that, for very small or large values of $(1 - D_{0r}^*)$, regular or singular perturbations methods can be used to obtain solutions to Eq. (9) for certain classes of orthotropic materials. In general, it is not easy to determine exact solutions to Eq. (9), although it can be inferred that the exact solutions should be in terms of hypergeometric functions of which Bessel functions are a subset. Fortunately, a number of approximate methods are available to solve Eq. (9) or its virtual work counterpart.

Boundary Conditions and the Approximate Solution

Two boundary conditions are considered in this analysis. They are 1) a clamped edge and 2) a simply supported edge. The free edge boundary condition is not considered because its uses seem to be very limited. As pointed out earlier, the essentially double eigenvalue problem posed in this paper seems to lack known exact closed-form solutions. Therefore, an approximate approach, in conjunction with the variational Hamilton's principles, is utilized to obtain the solutions. Polynomials are selected and test cases are calculated and compared to known "exact" results to determine the accuracy of the schematic. As the results shall indicate later, these polynomials proved to be so accurate that only the first two or three terms are used. In terms of the two eigenvalues, k_{0r} and ω_0 , the virtual work expression becomes

$$\delta U_{r_0} = \int_0^1 \delta \left\{ \left[\left(\frac{\partial^2 w}{\partial r_0^2} \right)^2 + 2 D_{0r}^* \epsilon_r \frac{1}{r_0} \frac{\partial w}{\partial r_0} \frac{\partial^2 w}{\partial r_0^2} + D_{0r}^* \left(\frac{1}{r_0} \frac{\partial w}{\partial r_0} \right)^2 + k_{0r} \left(\frac{\partial w}{\partial r_0} \right)^2 - \omega_0^2 w^2 \right] r_0 \right\} dr_0 \quad (12)$$

where k_{0r} is the affine buckling coefficient and ω_0 the affine frequency parameter.

Clamped Edge Plate

Consider the polynomial

$$W(r_0) = \sum_{n=0}^{\infty} \bar{a}_n (1 - r_0^2)^{n+2} \quad (13)$$

where

$$w(r_0, t) = W(r_0) e^{i\omega t} \quad (14)$$

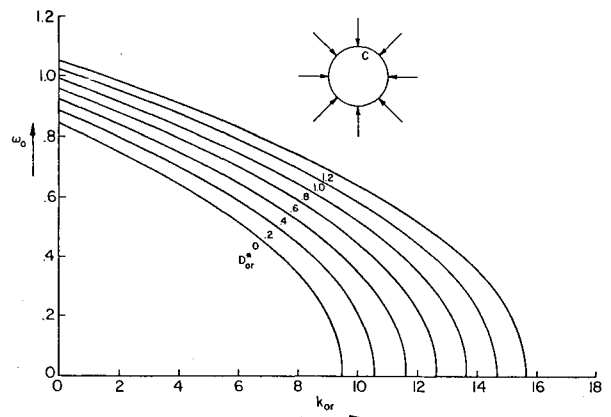


Fig. 1 The frequency parameter vs the stability coefficient of a circular orthotropic plate compressed on the clamped edge.

In accordance with the Ritz-Galerkin approach, Eq. (13) only satisfies the geometrical boundary conditions. Because of the accuracy of Eq. (13), the two terms used are given by

$$w(r_0, t) = [\bar{a}_0 (1 - r_0^2)^2 + \bar{a}_1 (1 - r_0^2)^3] e^{i\omega t} \quad (15)$$

When Eq. (15) is substituted into Eq. (12) and U_{r0} minimized with respect to \bar{a}_n ($n=1,2$), the condition for a nontrivial solution provides the double eigenvalue equation for the frequency and buckling given by

$$\omega_0^4 - 4.8(355 + 53D_{0r}^* - 8k_{0r})\omega_0^2 + 1008[(5 + 3D_{0r}^*)(23 + D_{0r}^*) + 1/5k_{0r}^2 - 2(7 + D_{0r}^*)k_{0r}] = 0 \quad (16)$$

Equation (16) is quadratic in both ω_0^2 and k_{0r} . Therefore, the standard method is used to determine the minimum values of these quantities. Thus, ω_0 is given by

$$\omega_0^2 = t_1 - (t_1^2 - 1008t_2)^{1/2} \quad (17)$$

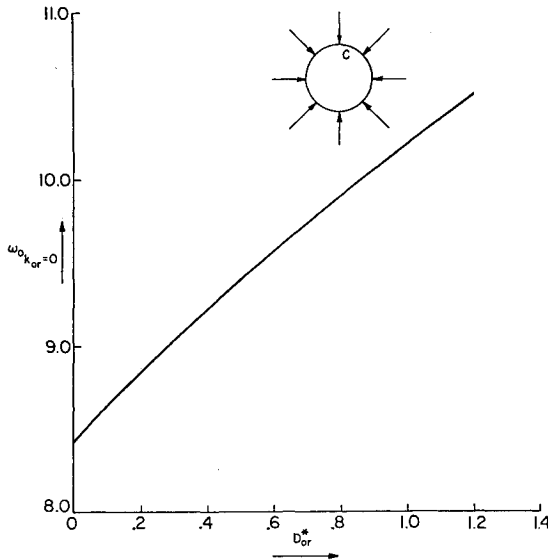


Fig. 2 The frequency parameter vs the generalized rigidity ratio of a circular orthotropic plate with clamped edge.

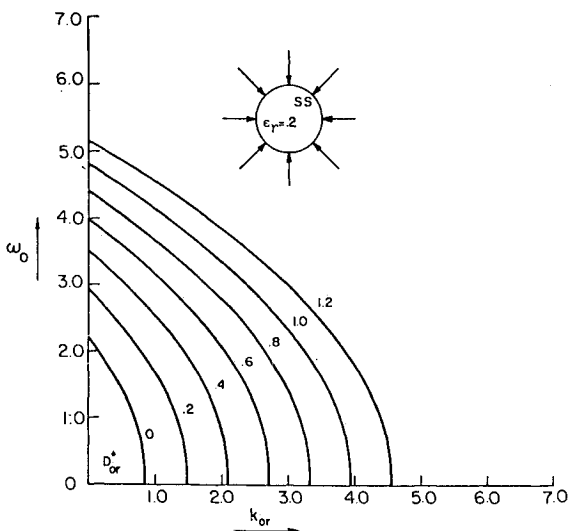


Fig. 3 The frequency parameter vs the stability coefficient of a circular orthotropic plate compressed on the hinged edge, $\epsilon_r = 0.2$.

where

$$t_1 \triangleq 2.4(355 + 53D_{0r}^* - 8k_{0r})$$

$$t_2 \triangleq (5 + 3D_{0r}^*)(23 + D_{0r}^*) + 1/5k_{0r}^2 - 2(7 + D_{0r}^*)k_{0r} \quad (18)$$

Equations (17) and (18), therefore, give the frequency parameter as a function of the midplane force for all plates with circular geometry and polar orthotropy. The affine buckling parameter for zero frequency is given by

$$k_{0r\omega_0=0} = 5(7 + D_{0r}^*) - [25(7 + D_{0r}^*)^2 - 5(5 + 3D_{0r}^*)(23 + D_{0r}^*)]^{1/2} \quad (19)$$

Equations (17-19) show a very good agreement with approximate results from Leissa,¹ and exact results from von Woinowsky-Krieger.⁴ Figures 1 and 2 illustrate the results for hypostiffened materials ($0 < D_{0r}^* \leq 1$), and one hyperstiffened material ($D_{0r}^* > 1$).

The empirical expressions derived for ω_0 and k_{0r} for fast applications are given by

$$\omega_{0k_{0r}=0} = 8.41 + 2D_{0r}^*, \quad 0 \leq D_{0r}^* \leq 0.4$$

$$= 8.522 + 1.72D_{0r}^*, \quad 0.4 \leq D_{0r}^* \leq 0.8$$

$$= 8.688 + 1.5125D_{0r}^*, \quad 0.8 \leq D_{0r}^* \leq 1.2 \quad (20)$$

$$k_{0r\omega_0=0} = 9.48 + 5.19D_{0r}^*, \quad 0 \leq D_{0r}^* \leq 1.2 \quad (21)$$

Simply Supported Plate

Consider the polynomial

$$W(r_0) = (1 - r_0) \sum_{n=0}^{\infty} \bar{a}_n r_0^n \quad (22)$$

By keeping the first three terms of Eq. (22) and substituting it into Eq. (12), an attempt to evaluate the resulting definite integrals reveals that a singularity exists at $r_0 = 0$. Elimination of this singularity results in a relationship between two of the three coefficients of the series. This in effect reduces the number of the independent coefficients to two. The resulting two-term polynomial is given by

$$w(r_0, t) = e^{i\omega t} (1 - r_0) (a_1 (1 + r_0) + a_2 r_0^2) \quad (23)$$

When Eq. (23) is substituted into Eq. (12) and U_{r0} is minimized with respect to \bar{a}_n ($n=1,2$), the condition for a nontrivial solution provides the frequency equation given by

$$\omega_0^4 - 35/3(114 + 24D_{0r}^*\epsilon_r + 15D_{0r}^* - 17/5k_{0r})\omega_0^2$$

$$+ 490[2/5k_{0r}^2 - (16 + 4D_{0r}^*\epsilon_r + D_{0r}^*)k_{0r}] + 4900/3$$

$$\times [4 + 12D_{0r}^*\epsilon_r + (13 + 6D_{0r}^*\epsilon_r)D_{0r}^* + (D_{0r}^*)^2] = 0 \quad (24)$$

Equation (24), which is quadratic in ω_0^2 and k_{0r} , is solved to obtain the following expression for the frequency parameter

$$\omega_0^2 = t_3 - (t_3^2 - 490t_4 - 4900/3t_5)^{1/2} \quad (25)$$

where

$$t_3 \triangleq 35/6(114 + 24D_{0r}^*\epsilon_r + 15D_{0r}^* - 17/5k_{0r})$$

$$t_4 \triangleq 2/5k_{0r}^2 - (16 + 4D_{0r}^*\epsilon_r + 3D_{0r}^*)k_{0r}$$

$$t_5 \triangleq 4 + 12D_{0r}^*\epsilon_r + (13 + 6D_{0r}^*\epsilon_r)D_{0r}^* + (D_{0r}^*)^2 \quad (26)$$

The presence of ϵ_r in Eq. (24) in contrast to Eq. (16) results from this parameter's absence and presence, respectively, in the clamped and hinged boundary terms in the equations of motion. Equations (25) and (26), therefore, express the frequency parameter in terms of the midplane force for all plates having circular geometry and polar orthotropy. The affine buckling parameter for zero frequency is given by the following,

$$k_{0r\omega_0=0} = t_6 - (t_6^2 - 25/3t_5)^{1/2} \quad (27)$$

where

$$t_6 \triangleq 5/4(16 + 4D_{0r}^* \epsilon_r + 3D_{0r}^*) \quad (28)$$

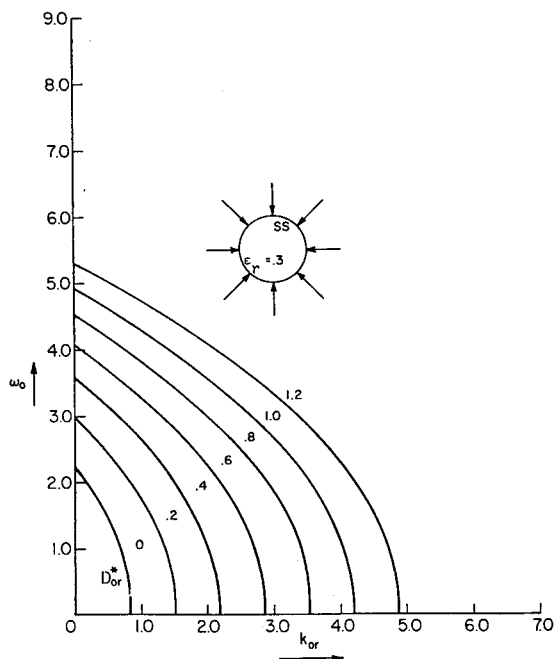


Fig. 4 The frequency parameter vs the stability coefficient of a circular orthotropic plate compressed on the hinged edge, $\epsilon_r = 0.3$.

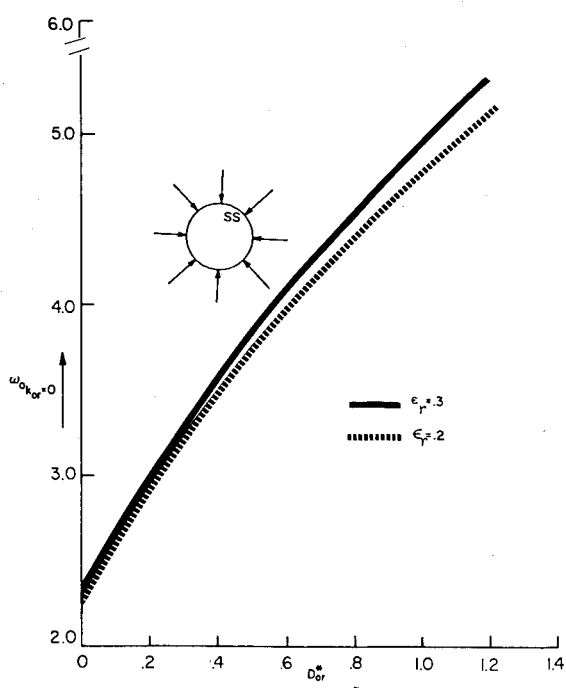


Fig. 5 The frequency parameter vs the generalized rigidity ratio of a circular orthotropic plate with hinged edge.

Equations (25-28) have been compared with results from Leissa,¹ Timoshenko and Gere,³ Lekhnitski,⁵ and Relton.⁷ The agreement is very good. Figures 3-5 depict the results for hypostiffened (and one hyperstiffened) plates using two values of the generalized Poisson's ratio. It is seen that both the frequency and buckling parameter increase with the generalized Poisson's ratio. This is a reverse of what was obtained for plates having rectangular geometry and orthotropy.¹¹⁻¹³

The empirical expressions derived for ω_0 and k_{0r} for fast applications are given by

$$k_{0r\omega_0=0} = 0.84 + 3.1D_{0r}^*; 0 \leq D_{0r}^* \leq 1.2; \epsilon_r = 0.2 \quad (29)$$

$$k_{0r\omega_0=0} = 0.84 + 3.36D_{0r}^*; 0 \leq D_{0r}^* \leq 1.2; \epsilon_r = 0.3 \quad (30)$$

$$\omega_{0k_{0r}=0}^2 = 35[19 + 3.3D_{0r}^* - (355.7 + 104.9D_{0r}^* + 7.96 \times (D_{0r}^*)^2)^{1/2}]; 0 \leq D_{0r}^* \leq 1.2; \epsilon_r = 0.2 \quad (31)$$

$$\omega_{0k_{0r}=0}^2 = 35[19 + 4.2D_{0r}^* - (355.7 + 137.4D_{0r}^* + 13.9 \times (D_{0r}^*)^2)^{1/2}]; 0 \leq D_{0r}^* \leq 1.2; \epsilon_r = 0.3 \quad (32)$$

Results

The results shown in Figs. 1-5 confirm some expected results and reveal some that are not so obvious. For example, both the frequency and buckling parameter decrease with increasing compressive force and, where applicable, increase with increasing generalized Poisson's ratio. The latter trend is a reverse of what was found for plates with rectangular geometry and orthotropy.

Concluding Remarks

This paper has attempted to study the vibrations of initially compressed plates having circular geometry and polar orthotropy in the affine space. A transformation of the physical equations of motion into the vibration trends for all materials can be carried out efficiently. Thus, using standing wave-type mode shapes in conjunction with the variational principles, simple algebraic expressions are obtained for the lowest symmetric frequencies. The effect of the midplane compressive forces, stiffness ratios, and the generalized Poisson's ratio on the frequencies are determined. Simpler (empirical) expressions for the frequencies for fast applications are also derived.

The major trends, which are two fold, confirm some expected results and reveal some that are not so obvious. For example, both the frequency and buckling parameter decrease with increasing compressive force, but increase with increasing generalized Poisson's ratio where applicable. This latter trend is the reverse of what was found by the authors^{12,13} for plates with rectangular geometry and orthotropy.

Acknowledgments

The work reported here was supported by a joint NASA/AFOSR Grant NGL33-018-003. The authors are very grateful to these agencies. We acknowledge useful discussions with Professors G. Handelman and W. Siegmund of Rensselaer Polytechnic Institute. We also thank Ms. McCurdy-Cyrus for her excellent typing.

References

1. Leissa, A. W., "Vibration of Plates," NASA SP-160, 1969.
2. Timoshenko, S. P. and Young, D. H., *Vibration Problems in Engineering*, D. Van Nostrand Co., Inc., Princeton, N.J., 1955.
3. Timoshenko, S. P. and Gere, J. M., *Theory of Elastic Stability*, McGraw-Hill Book Co., New York, 1961.

⁴von Woinowsky-Krieger, S., "Über Die Beulsicherheit von Kreisplatten mit kreiszylindrischer Aelotropie," *Ingenieur-Archiv*, 1958, pp. 129-133.

⁵Lekhnitski, S. G., *Anisotropic Plates*, American Iron and Steel Institute, New York, June 1956.

⁶Pandalai, K.A.V. and Patel, S. A., "Buckling of Orthotropic Circular Plates," *Journal of the Royal Aeronautical Society*, Vol. 69, pp. 279-280.

⁷Relton, R. E., *Applied Bessel Functions*, Dover Publications, New York, 1946.

⁸Handelman, G. and Cohen, H., "On the Effects of the Addition of Mass to Vibrating Systems," AFOSR TN 56-387, ASTIA Doc. No. 96045, Sept. 1956; also *Proceedings of the 9th International Congress on Applied Mechanics*, Vol. VII, 1957, pp. 509-518.

⁹Kantorovich, L. V. and Krylov, V. I., *Approximate Methods of Higher Analysis*, translated by C. D. Benster, Interscience, 1958.

¹⁰Brunelle, E. J., "The Use of a Double Affine Transformation to Obtain a Class of Generalized Elastodynamic Solutions of Orthotropic Plates," paper presented at the SIAM 1980 National Meeting, June 1980.

¹¹Oyibo, G. A., "The Use of Affine Transformations in the Analysis of Stability and Vibrations of Orthotropic Plates," Doctoral Thesis, Rennselaer Polytechnic Institute, May 1981.

¹²Brunelle, E. J., "Eigenvalue Similarity Rules for a Class of Rectangular Specially Orthotropic Laminated Plates," paper presented at the Ninth U.S. National Congress of Applied Mechanics, June 1982.

¹³Brunelle, E. J. and Oyibo, G. A., "Generic Buckling Curves for Specially Orthotropic Rectangular Plates," *AIAA Journal*, Vol. 21, Aug. 1983, pp. 1150-1156.

¹⁴Watson, G. N., *A Treatise on the Theory of Bessel Functions*, Macmillan, New York, 1944.

From the AIAA Progress in Astronautics and Aeronautics Series . . .

AEROTHERMODYNAMICS AND PLANETARY ENTRY—v. 77 HEAT TRANSFER AND THERMAL CONTROL—v. 78

Edited by A. L. Crosbie, University of Missouri-Rolla

The success of a flight into space rests on the success of the vehicle designer in maintaining a proper degree of thermal balance within the vehicle or thermal protection of the outer structure of the vehicle, as it encounters various remote and hostile environments. This thermal requirement applies to Earth-satellites, planetary spacecraft, entry vehicles, rocket nose cones, and in a very spectacular way, to the U.S. Space Shuttle, with its thermal protection system of tens of thousands of tiles fastened to its vulnerable external surfaces. Although the relevant technology might simply be called heat-transfer engineering, the advanced (and still advancing) character of the problems that have to be solved and the consequent need to resort to basic physics and basic fluid mechanics have prompted the practitioners of the field to call it thermophysics. It is the expectation of the editors and the authors of these volumes that the various sections therefore will be of interest to physicists, materials specialists, fluid dynamicists, and spacecraft engineers, as well as to heat-transfer engineers. Volume 77 is devoted to three main topics, Aerothermodynamics, Thermal Protection, and Planetary Entry. Volume 78 is devoted to Radiation Heat Transfer, Conduction Heat Transfer, Heat Pipes, and Thermal Control. In a broad sense, the former volume deals with the external situation between the spacecraft and its environment, whereas the latter volume deals mainly with the thermal processes occurring within the spacecraft that affect its temperature distribution. Both volumes bring forth new information and new theoretical treatments not previously published in book or journal literature.

Volume 77—444 pp., 6 × 9, illus., \$30.00 Mem., \$45.00 List

Volume 78—538 pp., 6 × 9, illus., \$30.00 Mem., \$45.00 List

TO ORDER WRITE: Publications Dept., AIAA, 1290 Avenue of the Americas, New York, N.Y. 10104